

1
2
3
4 **Blast Exposure Disrupts Tonotopic Frequency Map in the Primary**
5 **Auditory Cortex**
6
7
8
9

10
11 Samer Masri ¹, Li S. Zhang ², Hao Luo ³, Edward Pace ³, Jinsheng Zhang ^{3,4}, and Shaowen Bao
12 _{1,2}
13

14
15
16
17 1) Neuroscience Graduate Program and 2) Department of Physiology, University of Arizona,
18 Tucson, AZ 85724; 3) Department of Otolaryngology and 4) Department of Communication
19 Sciences & Disorders, Wayne State University, Detroit, MI 48201
20
21
22
23
24
25
26
27
28
29
30
31
32
33
34
35
36

37 Correspondence to: Shaowen Bao, Ph.D.
38 Department of Physiology
39 College of Medicine
40 University of Arizona
41 Tucson, AZ 85724-5051
42 E-mail: sbao@email.arizona.edu
43
44 Phone: (520) 621-5680
45
46
47
48
49
50
51
52
53
54
55
56
57
58
59
60
61
62
63
64
65

1
2
3
4 **ABSTRACT**
5

6
7 Blast exposure can cause various auditory disorders including tinnitus, hyperacusis, and other
8
9 central auditory processing disorders. While this is suggestive of pathologies in the central
10
11 auditory system, the impact of blast exposure on central auditory processing remains poorly
12
13 understood. Here we examined the effects of blast shockwaves on acoustic response properties
14
15 and frequency mapping in auditory cortex. We found that multiunits recording from the auditory
16
17 cortex exhibited higher acoustic thresholds and broader frequency tuning in blast-exposed
18
19 animals. Furthermore, there was distorted frequency mapping in primary auditory cortex. These
20
21 changes may contribute to central auditory processing disorders.
22
23
24
25
26
27
28

29 **KEYWORD:** blast, auditory cortex, frequency map, central auditory processing disorder,
30
31
32
33
34
35
36
37
38
39
40
41
42
43
44
45
46
47
48
49
50
51
52
53
54
55
56
57
58
59
60
61
62
63
64
65

INTRODUCTION

Exposure to blast shockwaves can cause sensory and neurological disorders in the auditory system, such as hearing loss, tinnitus, hyperacusis and central processing disorder (Jury and Flynn, 2001; Rossiter et al., 2006; Sayer et al., 2008; Belanger et al., 2009; Mao et al., 2012; Remenschneider et al., 2014; Saunders et al., 2015; Bressler et al., 2017; Ouyang et al., 2017). However, the mechanism by which blasts impact the auditory system remains unclear (Rosenfeld and Ford, 2010). Exposure to shockwaves causes damage to the ear, but the impact can be quite different from that of noise exposure (Bauer et al., 2008). Blast shockwaves are brief and often rupture the tympanic membrane, which decouples the inner ear from further mechanical over-stimulation (Xydakis et al., 2007). Consequently, blast exposure often causes severe acute hearing loss, but only mild long-term hearing loss following recovery of the tympanic membrane (Mao et al., 2012; Chen et al., 2013; Saunders et al., 2015; Bressler et al., 2017). By contrast, exposure to loud noises typically does not rupture the tympanic membrane, meaning that mechanical over-stimulation of the inner ear can be sustained, potentially resulting in more long-term hearing loss (Yang et al., 2011). Therefore, damage to hair cells, spiral ganglion neurons, and the central auditory pathway resulting from these distinctly different auditory traumas may vary greatly (Luo et al., 2014a, b; Niwa et al., 2016; Luo et al., 2017).

In addition to hearing loss, blasts cause traumatic brain injury (TBI) and may introduce additional pathologies to the central auditory pathway (Kamnaksh et al., 2011; Mao et al., 2012; Valiyaveetil et al., 2012; Tate et al., 2014; Race et al., 2017). Solid body structures, such as the brain, were previously considered to be at low-risk of sustaining shockwave injury (Argyros, 1997; Elsayed, 1997; Stuhmiller, 1997; Cernak et al., 2001). However, subsequent studies have

1
2
3
4 revealed a wide range of cellular injuries and inflammatory responses that occur despite a lack of
5
6 hemorrhage or gross brain damage (Cernak et al., 2001; Sajja et al., 2012; Abdul-Muneer et al.,
7
8 2013; Arun et al., 2013). For example, shockwaves from a single blast can compromise the
9
10 membranes of neural and glial cells, allowing intracellular proteins to leak into cerebrospinal
11
12 fluid (Saljo et al., 2003; Leung et al., 2008). Likewise, shockwave exposure activates resident
13
14 microglia and astrocytes within 30 minutes (Kaur et al., 1995; Cernak et al., 2001; Saljo et al.,
15
16 2001; Svetlov et al., 2010; Cernak et al., 2011; Du et al.) Activated microglia subsequently
17
18 release TNF- α and other pro-inflammatory cytokines, generating both acute and chronic cellular
19
20 inflammatory responses (Garden and Moller, 2006).
21
22
23
24
25
26
27

28 Here we examine the effects of blast shockwave exposure on auditory frequency mapping in the
29
30 primary auditory cortex (AI) of the rat. We found that blast exposure resulted in distorted
31
32 frequency mapping with over-representation of seemingly random narrow frequency ranges.
33
34
35
36
37

38 **MATERIAL AND METHODS**

39 *Animals.* All procedures used in this study were approved by the Animal Care and Use
40
41 Committees at the University of Arizona and Wayne State University. Ten Sprague-Daley rats,
42
43 male and 2-months old, were purchased from Charles River and used in this study. Five were
44
45 chosen randomly and assigned to the blast-exposed group and the remaining five rats were
46
47 assigned to the sham-exposed group.
48
49
50
51
52

53
54
55
56 *Blast exposure and behavioral tests.* Blast exposure was performed as described before (Mao et
57
58 al., 2012). The rat was anesthetized with isoflurane (0.75-1% in a 2:1 N₂O:O₂ gas mixture). The
59
60
61
62
63
64
65

1
2
3
4 right ear was protected with an earplug and sealed with mineral oil. Each rat was exposed to a
5
6 single 22-psi blast using a custom-built shock-tube assembly (ORA, Inc.). Blast exposure at this
7
8 level does not affect rats' eating and drinking behaviors. The pressure waveform was monitored
9
10 using piezoelectric sensors (PCB Piezotronics). A high-speed video camera (HG100K, Kodak),
11
12 which captures up to 3000 frames/s, was used to monitor the animal's orientation and movement,
13
14 prior to, during, and after delivery of the pressure wave. Sham-exposed animals underwent the
15
16 same procedure without blast delivery.
17
18
19
20
21
22

23
24 *Electrophysiological Recording Procedure.* AI in control and blast-exposed rats was mapped as
25
26 previously described (Kim and Bao, 2009). Rats were anesthetized with isoflurane (1-3%), and
27
28 placed on a homeothermic heating pad at 36.5 °C (Harvard Apparatus) in a sound attenuation
29
30 chamber. The head was secured with a custom head-holder that left the ears unobstructed. The
31
32 right auditory cortex was exposed and kept under a layer of silicone oil to prevent desiccation.
33
34 Multi-unit activity was evenly sampled from AI. AI can be identified by its tonotopic
35
36 orientation—higher frequencies are represented in a more rostral and dorsal position compared to
37
38 the caudally represented lower frequencies. Adjacent cortical auditory fields have different
39
40 tonotopic orientations (Guo et al., 2012). The border of AI was defined by unresponsive sites or
41
42 sites with CFs that were incongruent with the AI tonotopic gradient. As blast-exposed animals
43
44 tended to have incomplete representations of low and high frequencies (Figure 1), we carefully
45
46 searched for those representations near the rostral and caudal ends of AI in both blast-exposed
47
48 and sham-exposed animals. Neural responses were recorded using tungsten microelectrodes
49
50 (FHC) at a depth of 400-450 microns, presumably from the thalamorecipient layer. Responses to
51
52 25-ms tone pips (4-ms \cos^2 ramp) of 41 frequencies (2 to 32 kHz, 0.1 octave spacing) and eight
53
54
55
56
57
58
59
60
61
62
63
64
65

1
2
3
4 sound pressure levels (10–80 dB, 10-dB steps) were recorded three times per stimulus (i.e., a
5
6 frequency-intensity combination) to reconstruct the frequency-intensity receptive field. A TDT
7
8 coupler model electrostatic speaker was used to present all acoustic stimuli into the left ear
9
10 (contralateral to the recorded cortical hemisphere). All frequency-by-intensity combinations were
11
12 repeated 3 times.
13
14
15
16
17
18

19 An AI map was constructed from 19 to 46 multiunits from within AI (33 ± 5 sites, $n = 10$, mean
20
21 \pm SEM; please see Figure 1 for examples) out of a total of 40 to 68 multiunits that were recorded
22
23 (54 ± 5 sites, $n = 10$, mean \pm SEM) from each animal. When encountered, additional non-
24
25 responsive sites were marked on the cortical image to help define the boundary of AI, without
26
27 recording a receptive field.
28
29
30
31
32

33 Data Analysis. The receptive fields and response properties were calculated using custom
34
35 MATLAB programs as reported before (Yang et al., 2014). The three repetitions per stimulus are
36
37 not sufficient to determine statistically whether a multiunit responded to a particular frequency-
38
39 intensity combination. Therefore, we based our analysis on the entire receptive field, which was
40
41 reconstructed from responses to all 984 tone presentations. Briefly, a summed peri-stimulus time
42
43 histogram (PSTH) was generated from responses to all 984 tone pips (41 frequencies x 8
44
45 intensities x 3 repeats). The spontaneous firing rate of the multiunit was taken as the mean firing
46
47 rate in the 50-ms window prior to stimulus onset. Peak latency was defined as the time to the
48
49 peak PSTH response between 7 and 50 ms after the stimulus onset. The response window was
50
51 defined as the continuous period encompassing the PSTH peak, in which the mean firing rate in
52
53 every bin was higher than the baseline spontaneous firing rate. The onset latency was defined at
54
55
56
57
58
59
60
61
62
63
64
65

1
2
3
4 the onset of the response window, and the offset latency was defined at the end of the response
5
6 window. Spikes that occurred within the response window were counted to reconstruct the
7
8 receptive field.
9

10
11
12
13
14 The tuning curve contour was determined using a smoothing and thresholding algorithm
15
16 (for details and to see the effects of smoothing and thresholding, please see Figure 2 of Yang et
17
18 al., 2014). Briefly, the response magnitude was plotted in the frequency-intensity space, filtered
19
20 with a 3x3 mean filter, and thresholded at 35% of the maximum of the filtered response
21
22 magnitude. Response areas smaller than 5 pixels were considered noise and removed. The
23
24 contour of the suprathreshold area was used as the tuning curve. The raw responses in the
25
26 suprathreshold area was considered to be the isolated receptive field. The threshold of the neuron
27
28 was defined as the lowest sound level that elicited responses in the isolated receptive field. The
29
30 characteristic frequency (CF) of a neuron was defined as the center of mass of the isolated
31
32 receptive field (RF) for the two lowest suprathreshold sound levels. The maximum RF response
33
34 was the maximum number of spikes activated by a single frequency-intensity combination. The
35
36 mean and median RF response were the mean or median, respectively, number of spikes for all
37
38 frequency-intensity combinations within the receptive field. Tuning bandwidth (BW) was
39
40 defined as the bandwidth (on the logarithmic scale, in octaves) of the receptive field at the
41
42 specified intensity. We quantified BW at 80, 70 and 60 dB, but not at lower SPLs (< 60 dB)
43
44 because many neurons did not respond at those low levels. To accurately quantify BW at low
45
46 SPLs, we also measured BW at 10, 20 and 30 dB above the threshold. The receptive field size
47
48 was the number of frequency-intensity combinations within the receptive field.
49
50
51
52
53
54
55
56

57 AI space was tessellated (with the voronoi function in MATLAB) into polygons, and
58
59
60
61
62
63
64
65

1
2
3
4 each polygon was assigned the response properties of the corresponding recording site to
5
6 generate auditory cortical maps.
7
8
9

10
11 Statistics. Unless otherwise stated in the text, statistical significance was determined with
12
13 ANOVAs with post hoc Bonferroni's test. All response properties were averaged for each animal
14
15 and compared between groups. Results were presented as mean \pm SEM.
16
17
18
19
20

21 RESULTS

22
23
24 The cortical frequency map in AI was examined in blast- and sham-exposed animals 3 months
25
26 after the exposure. AI frequency maps of sham-exposed animals were tonotopically organized,
27
28 with all frequencies approximately equally represented in each animal (one-sample Kolmogorov-
29
30 Smirnov test against a log-uniform distribution from 2 kHz to 32 kHz, $p > 0.1$; for example, see
31
32 **Figure 1**, Z-3 and Z-14). By contrast, all blast-exposed animals had a large area in AI that over-
33
34 represented a relatively narrow frequency band (Kolmogorov-Smirnov test, $p < 0.001$; **Figure 1**).
35
36 Two animals had over-representations of low frequencies (e.g., Z-12 in **Figure 1**), two over-
37
38 represented middle frequencies (e.g., Z-7 in **Figure 1**) and one over-represented high frequencies
39
40 (Z-5 in **Figure 1**).
41
42
43
44
45
46
47
48

49 Inspection of receptive fields (**Figure 2**) suggests substantial differences in neuronal response
50
51 properties, such as tuning bandwidth and sound threshold. Quantitative analysis indicates that AI
52
53 neurons in the blast-exposed animals had higher thresholds than those of the sham-exposed
54
55 animals (one-way ANOVA, $F_{1,8} = 5.97$, $p = 0.040$; **Figure 3**). This is consistent with a high ABR
56
57 threshold in the blast- compared to the sham-exposed animals (Luo et al., 2014b).
58
59
60
61
62
63
64
65

1
2
3
4
5
6
7 We plotted threshold maps (**Figure 4**) to illustrate the topographic organization of the neuronal
8
9 response threshold. While blast-exposed animals had higher thresholds in general compared to
10
11 the sham-exposed group (see **Figure 3**), the range of frequencies with higher thresholds within a
12
13 map appeared to be variable for the blast-exposed animals. Furthermore, neuronal response
14
15 threshold changes do not appear to be correlated with expansions of frequency representation.
16
17 For example, Z-7 and Z-12 had higher thresholds in the expanded frequency ranges compared to
18
19 other frequency ranges (i.e., fewer blue sites; see **Figure 4**), whereas Z-5 had lower thresholds in
20
21 the expanded frequency range relative to other frequency ranges (more blue sites; the expanded
22
23 frequency ranges in the blast-exposed animals are shown in **Figure 1**).

24
25
26
27
28
29
30
31 We measured two types of tuning bandwidths—tuning bandwidth at specified sound levels, and
32
33 tuning bandwidth at intensities relative to the intensity threshold. The results indicate that
34
35 bandwidth was significantly broadened at 50 and 60 dB SPL (**Figure 5**; Group x Sound-level
36
37 two-way ANOVA; Group effect, $F_{1,24} = 15.01$, $p < 0.001$; Sound level effect, $F_{2,24} = 10.21$, $p <$
38
39 0.001 ; Post Hoc test, $p < 0.05$ at 50 and 60 dB SPL), and at 20 and 30 dB above the intensity
40
41 threshold for AI neurons in the blast-exposed animals compared to sham-exposed animals
42
43 (Group x Sound-level two-way ANOVA; Group effect, $F_{1,24} = 13.11$, $p = 0.0014$; Sound level
44
45 effect, $F_{2,24} = 24.64$, $p < 0.001$; Post Hoc test, $p < 0.05$ at 20 and 30 dB above threshold). In
46
47 addition, the onset, peak, and offset latency of the cortical responses to tonal stimulus are
48
49 significantly shorter in the blast-exposed animals compared to controls (**Figure 6**; Mann-
50
51 Whitney test $n_1 = n_2 = 5$: onset, $U = 2.50$, $p = 0.035$; peak, $U = 1.00$, $p = 0.016$; offset $U = 0.001$,
52
53
54
55
56
57
58 $p = 0.009$).

1
2
3
4
5
6
7 We measured spontaneous activity as the mean number of spikes in the 50-ms window right
8
9 before the onset of the tonal stimulus, and found no difference between the control and the blast-
10
11 exposed groups (**Figure 7**, ANOVA, $F_{1,8} = 0.065$, $p = 0.81$). We also measured median, mean
12
13 and maximum responses of cortical neurons to tones in the frequency-intensity response area.
14
15 There were no differences in either of these measures between the blast-exposed and the control
16
17 groups (**Figure 7**, ANOVA, $p > 0.5$ for all measures).
18
19
20
21
22

23 **DISCUSSION**

24
25
26 In this study we have shown that blast exposure disrupts the AI frequency map and changes
27
28 neuronal response properties. Some of these changes are similar to those observed in animals
29
30 following noise exposure. For example, the increased response threshold and shortened response
31
32 latencies observed in this study have previously been reported following noise exposure (Gallo
33
34 and Glorig, 1964; Syka and Rybalko, 2000; Norena et al., 2003). Noise exposure often results in
35
36 hearing loss in a limited frequency range, causing a shift of neuronal tuning away from the
37
38 hearing loss frequencies and towards the neighboring frequencies. The consequent map
39
40 reorganization typically manifests as expanded representation of the frequencies flanking the
41
42 hearing loss frequency range (Yang et al., 2011).
43
44
45
46
47
48
49

50
51 The blast exposure procedure used in this study has been previously shown to cause TBI (Mao et
52
53 al., 2012). TBI typically elevates the expression of pro-inflammatory cytokines in the brain
54
55 (Berpohl et al., 2007), which in turn modulate neuronal functions such as synaptic transmission
56
57 and membrane excitability. For example, TBI often increases TNF- α expression (Berpohl et al.,
58
59
60
61
62
63
64
65

1
2
3
4 2007), and TNF- α increases the excitation-to-inhibition ratio by enhancing excitatory synapses
5
6 and weakening inhibitory synapses (Beattie et al., 2002; Stellwagen and Malenka, 2006). This
7
8 process could lead to amplification of small differences in the level of (possibly hidden) hearing
9
10 loss across different frequencies, resulting in disproportional AI map reorganization.
11
12
13
14

15
16 One observation in the present study that deviated from previous reports (Luo et al., 2017) is the
17
18 lack of changes in AI neural activity and responses (**Figure 7**). Noise and blast exposure have
19
20 previously been shown to increase spontaneous and sound-evoked activity in the auditory cortex
21
22 (Eggermont and Roberts, 2004; Kotak et al., 2005; Luo et al., 2017). However, we did not
23
24 observe those types of changes. This may be due to the differences in experimental preparation
25
26 and recording conditions. We recorded cortical multiunit activity in acute preparation, from
27
28 anesthetized animals, and we compared activity between different animals. A better way to
29
30 compare neural activity is through chronic recording of single unit activity in awake animals
31
32 before and after blast exposure. It is also possible that changes in AI neural activity occur in a
33
34 specific time window following blast exposure, and that our experiment took place after the
35
36 activity had recovered. This could also be addressed by using chronic recording of neuronal
37
38 activity to track activity changes. A third possibility is that blast-induced TBI and hearing loss
39
40 have opposite effects on neuronal activity. If so, we may observe an increase, no change, or a
41
42 decrease in spontaneous and evoked activity depending on the type and degree of TBI and/or
43
44 hearing loss.
45
46
47
48
49
50
51
52
53
54

55 Blasts cause hearing loss and TBI, both of which are related to tinnitus. Hearing loss is the
56
57 largest risk factor for tinnitus (Nondahl et al., 2002; Nelson and Chen, 2004). It disrupts
58
59
60
61
62
63
64
65

1
2
3
4 excitation-inhibition balance, and increases spontaneous, synchronous, and/or burst firing in the
5
6 central auditory pathway (Seki and Eggermont, 2003; Kotak et al., 2005; Eggermont, 2007).
7
8 These changes in central auditory activity have been considered potential mechanisms
9
10 underlying tinnitus (Eggermont and Roberts, 2004). Traumatic brain injury (TBI), such as what
11
12 results from blast exposure, is also a significant risk factor for tinnitus (Vernon and Press, 1994;
13
14 Folmer and Griest, 2003; Lew and Guillory, 2007). For example, the incidence of tinnitus is
15
16 higher in military personnel with TBI compared to those without TBI, with up to 38% of
17
18 veterans suffering from TBI also experiencing tinnitus (Lew and Guillory, 2007). TBI-triggered
19
20 increases in the pro-inflammatory cytokine TNF- α may increase the excitation-to-inhibition ratio
21
22 (Beattie et al., 2002; Stellwagen and Malenka, 2006) and increase the incidence of tinnitus.
23
24 Sensory map reorganization has been proposed as a potential mechanism underlying tinnitus
25
26 (Eggermont, 2006; Engineer et al., 2011). Such a notion seems to be supported by our
27
28 observation that AI frequency mapping was disrupted by blast exposure. Blasts may cause
29
30 central auditory processing disorder in the absence of hearing threshold increases, such as
31
32 difficulty listening in noisy environment (Saunders et al., 2015; Bressler et al., 2017). Disrupted
33
34 auditory frequency maps may contribute to this pathological condition. Further studies are
35
36 needed to determine a causal relationship between the two blast-caused pathologies.
37
38
39
40
41
42
43
44
45
46
47
48

49 **ACKNOWLEDGEMENT:** The research was supported by Department of Defense
50
51 (W81XWH-11-2-0031). We thank Alexander K. Zinsmaier for comments on the manuscript.
52
53
54
55
56
57
58
59
60
61
62
63
64
65

1
2
3
4 **FIGURES**
5
6

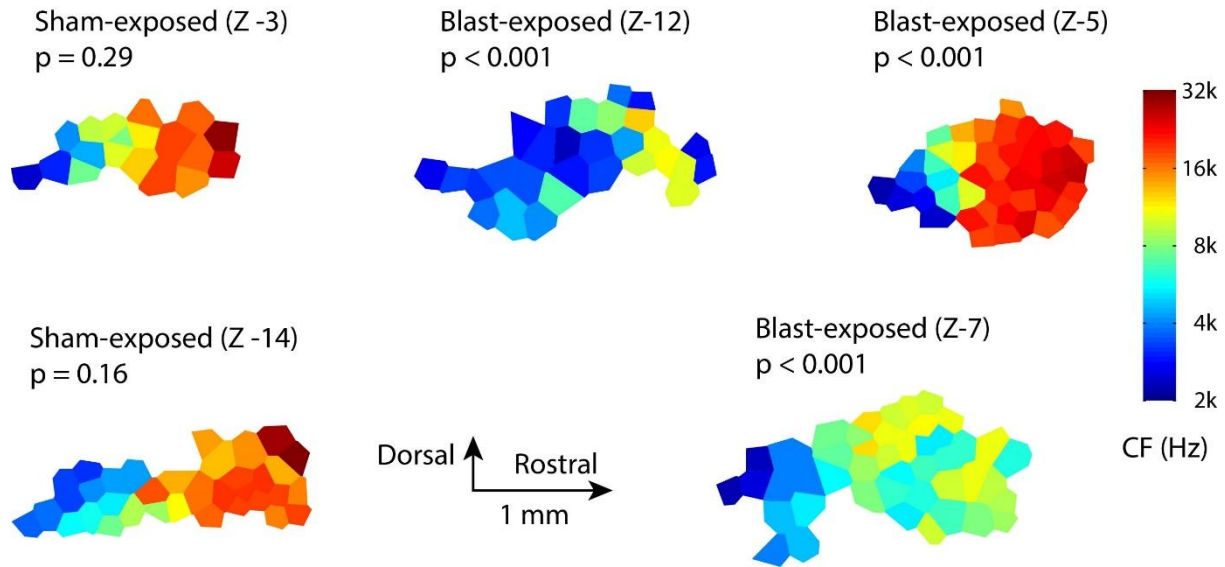
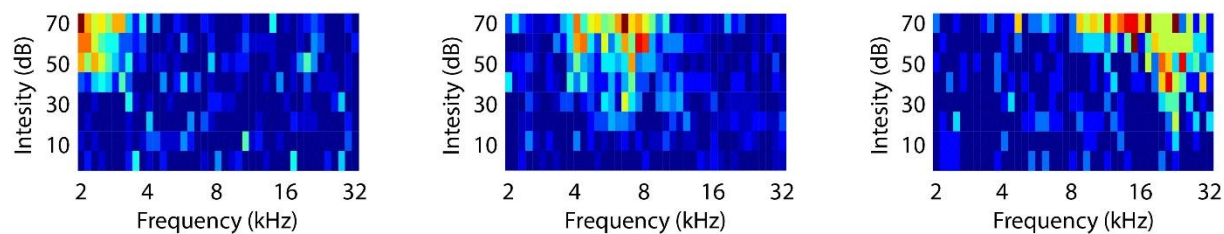
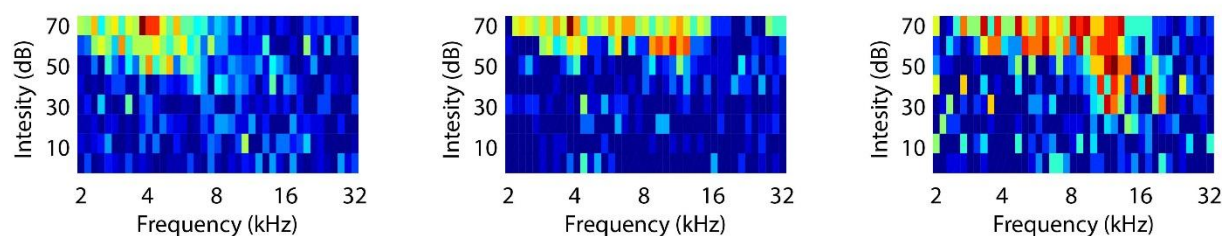


Figure 1. Representative cortical frequency maps showing disrupted cortical map in blast-exposed animals. Control maps (Z-3 and Z-14) showed tonotopic representation of the complete frequency spectrum from 2-4 kHz to 32 kHz. By contrast, maps from blast-exposed animals showed disproportionately large representations of seemingly random and narrower frequency ranges. For example, Z-12 had enlarged representations of low frequencies (blue colors), Z-7 had enlarged representations of middle frequencies (blue and yellow colors) and Z-5 had enlarged representation of high frequencies (red colors). The p values are presented for one-sample Kolmogorov-Smirnov tests against a log-uniform distribution from 2 kHz to 32 kHz.

1
2
3
4
5
6 Sham-exposed
7
8



19 Blast-exposed
20
21



33 **Figure 2. Representative receptive fields from control and blast-exposed animals.** Receptive field
34 from blasted animals are generally more broadly tuned, and with a higher threshold. Horizontal axis
35 depicts frequency from 2 to 32 kHz with 0.1 octaves steps. Vertical axis depict intensity from 0 to 80
36 dB SPL with 10 dB steps.
37
38
39
40
41
42
43
44
45
46
47
48
49
50
51
52
53
54
55
56
57
58
59
60
61
62
63
64
65

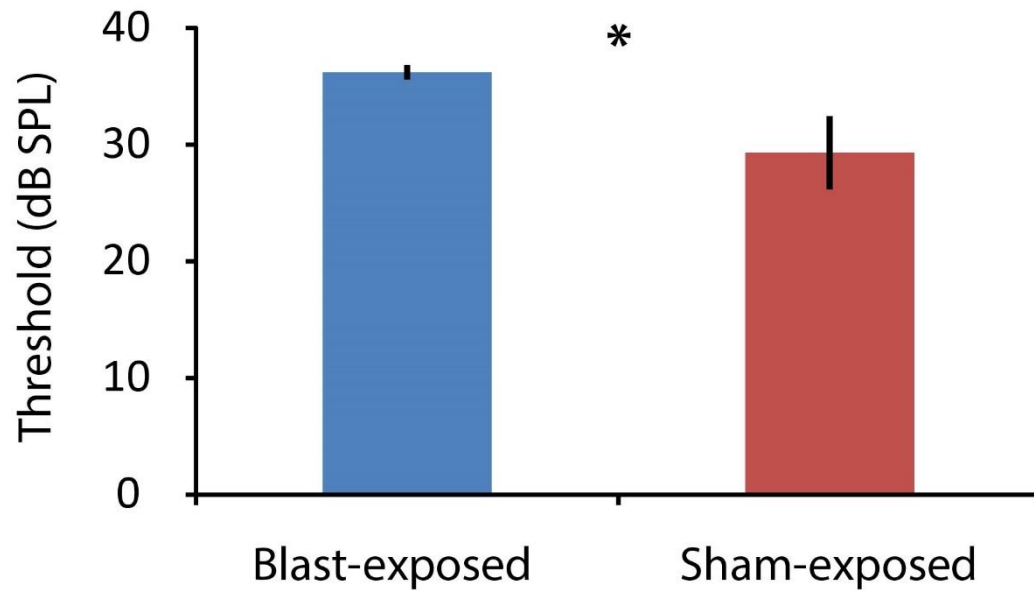


Figure 3. Intensity threshold was elevated for blast-exposed animals. Error bars represent SEM and * indicates $p < 0.05$.

1
2
3
4
5
6
7
8
9
10
11
12
13
14
15
16
17
18
19
20
21
22
23
24
25
26
27
28
29
30
31
32
33
34
35
36
37
38
39
40
41
42
43
44
45
46
47
48
49
50
51
52
53
54
55
56
57
58
59
60
61
62
63
64
65

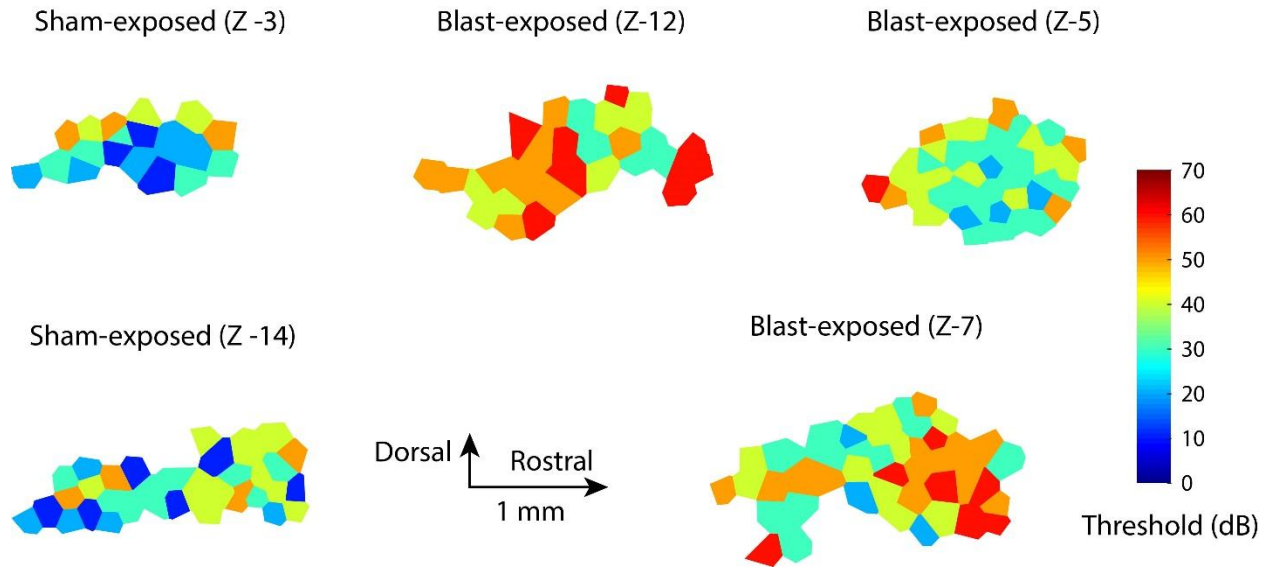


Figure 4. Representative cortical threshold maps showing elevated sound threshold in blast-exposed animals. Control maps (Z-3 and Z-14) showed low response thresholds at most of the recorded sites. By contrast, maps from blast-exposed animals showed middle and high thresholds at most of the recorded sites. These maps were from the same animals as those in Figure 1.

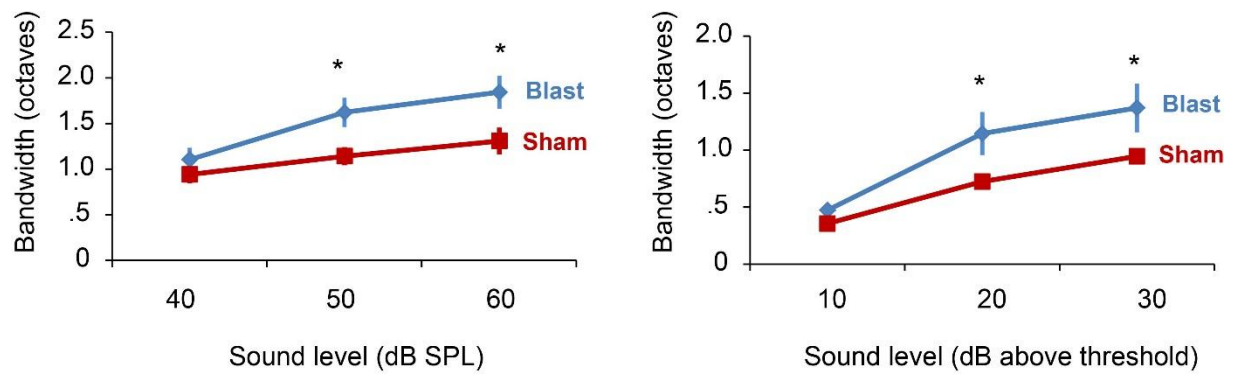


Figure 5. Cortical tuning bandwidths were elevated in blast-exposed animals. Blue: blast-exposed group (n = 5); red: control group (n = 5). Error bars represent SEM. * indicates p < 0.05.

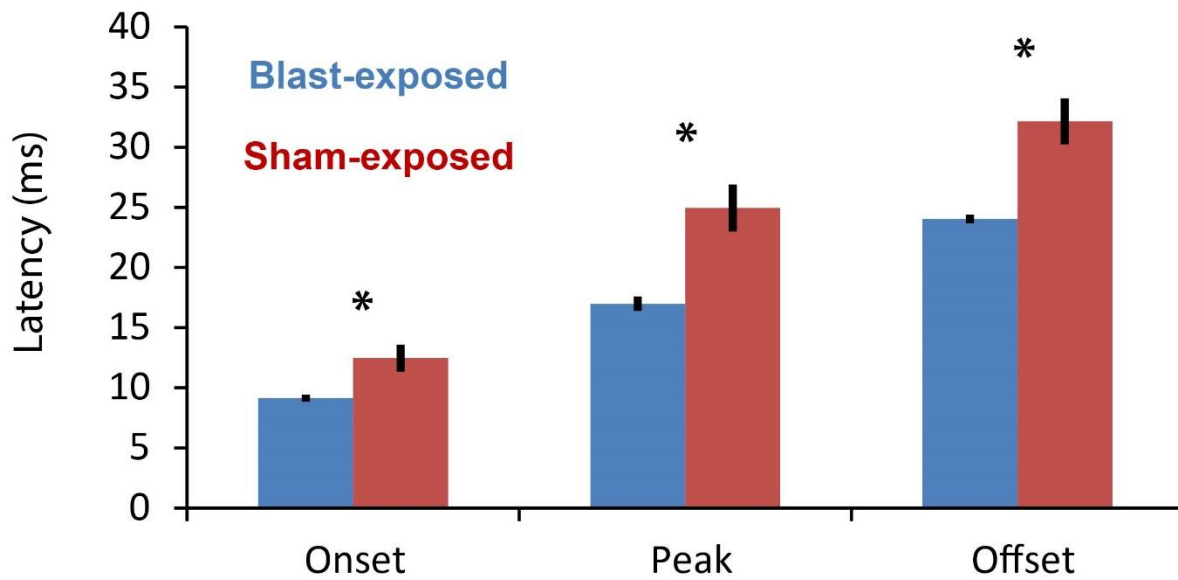


Figure 6. Onset, peak and offset latencies of the cortical responses were significantly reduced in blast-exposed animals. Blue: blast-exposed group (n = 5) ; red: control group (n = 5). Error bars represent SEM. * indicates $p < 0.05$.

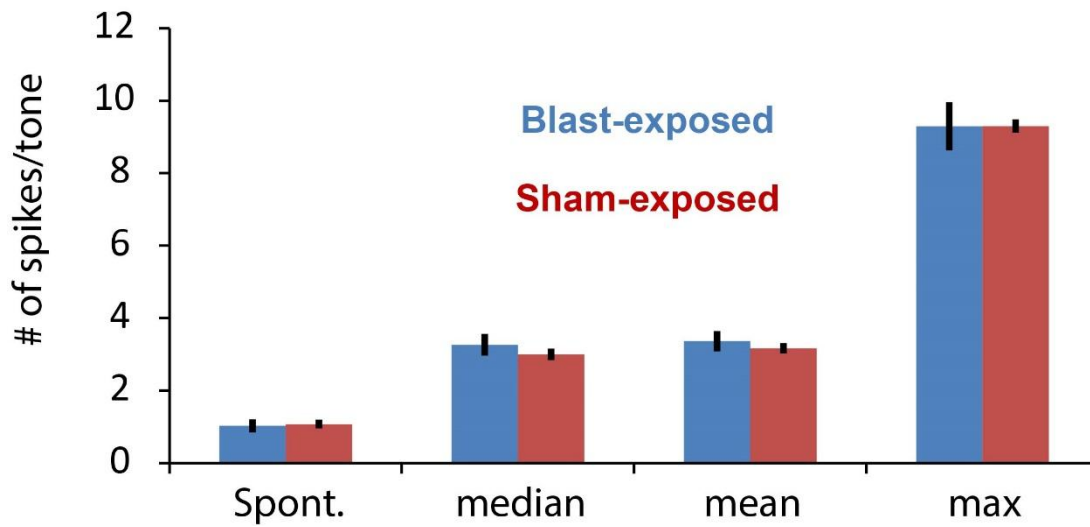


Figure 7. There were no differences in spontaneous activity, or median, mean or maximum response to tones between the control and the blast-exposed groups. Blue: blast-exposed group; red: control group. The two groups were not significantly different in any of the measures. Error bars represent SEM.

REFERENCES

- Abdul-Muneer PM, Schuetz H, Wang F, Skotak M, Jones J, Gorantla S, Zimmerman MC, Chandra N, Haorah J (2013) Induction of oxidative and nitrosative damage leads to cerebrovascular inflammation in an animal model of mild traumatic brain injury induced by primary blast. *Free Radical Biology and Medicine* 60:282-291.
- Argyros GJ (1997) Management of primary blast injury. *Toxicology* 121:105-115.
- Arun P, Abu-Taleb R, Oguntayo S, Wang Y, Valiyaveetil M, Long JB, Nambiar MP (2013) Acute mitochondrial dysfunction after blast exposure: potential role of mitochondrial glutamate oxaloacetate transaminase. *Journal of neurotrauma* 30:1645-1651.
- Bauer CA, Turner JG, Caspary DM, Myers KS, Brozoski TJ (2008) Tinnitus and inferior colliculus activity in chinchillas related to three distinct patterns of cochlear trauma. *Journal of neuroscience research* 86:2564-2578.
- Beattie EC, Stellwagen D, Morishita W, Bresnahan JC, Ha BK, Von Zastrow M, Beattie MS, Malenka RC (2002) Control of synaptic strength by glial TNF α . *Science* 295:2282-2285.
- Belanger HG, Kretzmer T, Yoash-Gantz R, Pickett T, Tupler LA (2009) Cognitive sequelae of blast-related versus other mechanisms of brain trauma. *Journal of the International Neuropsychological Society* 15:1-8.
- Berpohl D, You Z, Lo EH, Kim HH, Whalen MJ (2007) TNF α and Fas mediate tissue damage and functional outcome after traumatic brain injury in mice. *J Cereb Blood Flow Metab* 27:1806-1818.
- Bressler S, Goldberg H, Shinn-Cunningham B (2017) Sensory coding and cognitive processing of sound in Veterans with blast exposure. *Hear Res* 349:98-110.
- Cernak I, Wang Z, Jiang J, Bian X, Savic J (2001) Ultrastructural and functional characteristics of blast injury-induced neurotrauma. *Journal of Trauma and Acute Care Surgery* 50:695-706.
- Cernak I, Merkle AC, Koliatsos VE, Bilik JM, Luong QT, Mahota TM, Xu L, Slack N, Windle D, Ahmed FA (2011) The pathobiology of blast injuries and blast-induced neurotrauma as identified using a new experimental model of injury in mice. *Neurobiol Dis* 41:538-551.
- Chen W, Wang J, Chen J, Chen J, Chen Z (2013) Relationship between changes in the cochlear blood flow and disorder of hearing function induced by blast injury in guinea pigs. *International journal of clinical and experimental pathology* 6:375.
- Du X, West MB, Cai Q, Cheng W, Ewert DL, Li W, Floyd RA, Kopke RD (2017) Antioxidants reduce neurodegeneration and accumulation of pathologic Tau proteins in the auditory system after blast exposure. *Free Radic Biol Med* 108:627-643.
- Eggermont JJ (2006) Cortical tonotopic map reorganization and its implications for treatment of tinnitus. *Acta Otolaryngol Suppl*:9-12.
- Eggermont JJ (2007) Correlated neural activity as the driving force for functional changes in auditory cortex. *Hearing research* 229:69-80.
- Eggermont JJ, Roberts LE (2004) The neuroscience of tinnitus. *Trends in neurosciences* 27:676-682.
- Elsayed NM (1997) Toxicology of blast overpressure. *Toxicology* 121:1-15.
- Engineer ND, Riley JR, Seale JD, Vrana WA, Shetake JA, Sudanagunta SP, Borland MS, Kilgard MP (2011) Reversing pathological neural activity using targeted plasticity. *Nature* 470:101-104.
- Folmer RL, Griest SE (2003) Chronic tinnitus resulting from head or neck injuries. *Laryngoscope* 113:821-827.
- Gallo R, Glorig A (1964) Permanent threshold shift changes produced by noise exposure and aging. *American Industrial Hygiene Association Journal* 25:237-245.

- 1
2
3
4 Garden GA, Moller T (2006) Microglia biology in health and disease. *J Neuroimmune Pharmacol* 1:127-
5 137.
6
7 Guo W, Chambers AR, Darrow KN, Hancock KE, Shinn-Cunningham BG, Polley DB (2012) Robustness of
8 cortical topography across fields, laminae, anesthetic states, and neurophysiological signal types.
9 *J Neurosci* 32:9159-9172.
10
11 Jury MA, Flynn MC (2001) Auditory and vestibular sequelae to traumatic brain injury: a pilot study. *The*
12 *New Zealand Medical Journal* 114:286-288.
13
14 Kamnaksh A, Kovesdi E, Kwon SK, Wingo D, Ahmed F, Grunberg NE, Long J, Agoston DV (2011) Factors
15 affecting blast traumatic brain injury. *J Neurotrauma* 28:2145-2153.
16
17 Kaur C, Singh J, Lim MK, Ng BL, Yap EP, Ling EA (1995) The response of neurons and microglia to blast
18 injury in the rat brain. *Neuropathol Appl Neurobiol* 21:369-377.
19
20 Kim H, Bao S (2009) Selective increase in representations of sounds repeated at an ethological rate. *J*
21 *Neurosci* 29:5163-5169.
22
23 Kotak VC, Fujisawa S, Lee FA, Karthikeyan O, Aoki C, Sanes DH (2005) Hearing loss raises excitability in
24 the auditory cortex. *Journal of Neuroscience* 25:3908-3918.
25
26 Leung LY, VandeVord PJ, Dal Cengio AL, Bir C, Yang KH, King AI (2008) Blast related neurotrauma: a
27 review of cellular injury. *Mol Cell Biomech* 5:155-168.
28
29 Lew HL, Guillory SB (2007) Auditory dysfunction in traumatic brain injury. *Journal of rehabilitation*
30 *research and development* 44:921.
31
32 Luo H, Pace E, Zhang J (2017) Blast-induced tinnitus and hyperactivity in the auditory cortex of rats.
33 *Neuroscience* 340:515-520.
34
35 Luo H, Pace E, Zhang X, Zhang J (2014a) Blast-induced tinnitus and spontaneous activity changes in the
36 rat inferior colliculus. *Neurosci Lett* 580:47-51.
37
38 Luo H, Pace E, Zhang X, Zhang J (2014b) Blast-Induced tinnitus and spontaneous firing changes in the
39 dorsal cochlear nucleus. *J Neurosci Res* 92:1466-1477.
40
41 Mao JC, Pace E, Pierozynski P, Kou Z, Shen Y, VandeVord P, Haacke EM, Zhang X, Zhang J (2012) Blast-
42 induced tinnitus and hearing loss in rats: behavioral and imaging assays. *Journal of neurotrauma*
43 29:430-444.
44
45 Nelson JJ, Chen K (2004) The relationship of tinnitus, hyperacusis, and hearing loss. *Ear, nose & throat*
46 *journal* 83:472.
47
48 Niwa K, Mizutani K, Matsui T, Kurioka T, Matsunobu T, Kawauchi S, Satoh Y, Sato S, Shiotani A, Kobayashi
49 Y (2016) Pathophysiology of the inner ear after blast injury caused by laser-induced shock wave.
50 *Sci Rep* 6:31754.
51
52 Nondahl DM, Cruickshanks KJ, Wiley TL, Klein R, Klein BE, Tweed TS (2002) Prevalence and 5-year
53 incidence of tinnitus among older adults: the epidemiology of hearing loss study. *Journal of the*
54 *American Academy of Audiology* 13:323-331.
55
56 Norena AJ, Tomita M, Eggermont JJ (2003) Neural changes in cat auditory cortex after a transient pure-
57 tone trauma. *J Neurophysiol* 90:2387-2401.
58
59 Ouyang J, Pace E, Lepczyk L, Kaufman M, Zhang J, Perrine SA, Zhang J (2017) Blast-Induced Tinnitus and
60 Elevated Central Auditory and Limbic Activity in Rats: A Manganese-Enhanced MRI and
61 Behavioral Study. *Sci Rep* 7:4852.
62
63 Race N, Lai J, Shi R, Bartlett EL (2017) Differences in post-injury auditory system pathophysiology after
64 mild blast and non-blast acute acoustic trauma. *J Neurophysiol*:jn 00710 02016.
65
66 Remenschneider AK, Lookabaugh S, Aliphas A, Brodsky JR, Devaiah AK, Dagher W, Grundfast KM,
67 Heman-Ackah SE, Rubin S, Sillman J, Tsai AC, Vecchiotti M, Kujawa SG, Lee DJ, Quesnel AM (2014)
68 Otologic outcomes after blast injury: the Boston Marathon experience. *Otol Neurotol* 35:1825-
69 1834.

- 1
2
3
4 Rosenfeld JV, Ford NL (2010) Bomb blast, mild traumatic brain injury and psychiatric morbidity: a review.
5 Injury 41:437-443.
6
7 Rossiter S, Stevens C, Walker G (2006) Tinnitus and its effect on working memory and attention. Journal
8 of speech, language, and hearing research 49:150-160.
9
10 Sajja VSSS, Galloway MP, Ghoddoussi F, Thiruthalinathan D, Kepsel A, Hay K, Bir CA, VandeVord PJ (2012)
11 Blast - induced neurotrauma leads to neurochemical changes and neuronal degeneration in the
12 rat hippocampus. NMR in biomedicine 25:1331-1339.
13
14 Saljo A, Huang YL, Hansson HA (2003) Impulse noise transiently increased the permeability of nerve and
15 glial cell membranes, an effect accentuated by a recent brain injury. J Neurotrauma 20:787-794.
16
17 Saljo A, Bao F, Hamberger A, Haglid KG, Hansson HA (2001) Exposure to short-lasting impulse noise
18 causes microglial and astroglial cell activation in the adult rat brain. Pathophysiology 8:105-111.
19
20 Saunders GH, Frederick MT, Arnold M, Silverman S, Chisolm TH, Myers P (2015) Auditory difficulties in
21 blast-exposed Veterans with clinically normal hearing. J Rehabil Res Dev 52:343-360.
22
23 Sayer NA, Chiros CE, Sigford B, Scott S, Clothier B, Pickett T, Lew HL (2008) Characteristics and
24 rehabilitation outcomes among patients with blast and other injuries sustained during the
25 Global War on Terror. Archives of physical medicine and rehabilitation 89:163-170.
26
27 Seki S, Eggermont JJ (2003) Changes in spontaneous firing rate and neural synchrony in cat primary
28 auditory cortex after localized tone-induced hearing loss. Hearing research 180:28-38.
29
30 Stellwagen D, Malenka RC (2006) Synaptic scaling mediated by glial TNF-alpha. Nature 440:1054-1059.
31
32 Stuhmiller JH (1997) Biological response to blast overpressure: a summary of modeling. Toxicology
33 121:91-103.
34
35 Svetlov SI, Prima V, Kirk DR, Gutierrez H, Curley KC, Hayes RL, Wang KK (2010) Morphologic and
36 biochemical characterization of brain injury in a model of controlled blast overpressure
37 exposure. J Trauma 69:795-804.
38
39 Syka J, Rybalko N (2000) Threshold shifts and enhancement of cortical evoked responses after noise
40 exposure in rats. Hearing research 139:59-68.
41
42 Tate DF, York GE, Reid MW, Cooper DB, Jones L, Robin DA, Kennedy JE, Lewis J (2014) Preliminary
43 findings of cortical thickness abnormalities in blast injured service members and their
44 relationship to clinical findings. Brain Imaging Behav 8:102-109.
45
46 Valiyaveetil M, Alamneh Y, Miller SA, Hammamieh R, Wang Y, Arun P, Wei Y, Oguntayo S, Nambiar MP
47 (2012) Preliminary studies on differential expression of auditory functional genes in the brain
48 after repeated blast exposures. J Rehabil Res Dev 49:1153-1162.
49
50 Vernon JA, Press LS (1994) Characteristics of tinnitus induced by head injury. Arch Otolaryngol Head
51 Neck Surg 120:547-551.
52
53 Xydakis MS, Bebarta VS, Harrison CD, Conner JC, Grant GA, Robbins AS (2007) Tympanic-membrane
54 perforation as a marker of concussive brain injury in Iraq. New England Journal of Medicine
55 357:830-831.
56
57 Yang S, Weiner BD, Zhang LS, Cho SJ, Bao S (2011) Homeostatic plasticity drives tinnitus perception in an
58 animal model. Proc Natl Acad Sci U S A 108:14974-14979.
59
60 Yang S, Zhang LS, Gibboni R, Weiner B, Bao S (2014) Impaired development and competitive refinement
61 of the cortical frequency map in tumor necrosis factor-alpha-deficient mice. Cereb Cortex
62 24:1956-1965.
63
64
65